Environmental Science & Technology

Article

Cite This: Environ. Sci. Technol. 2019, 53, 354−364

pubs.acs.org/est

Biocatalytic Degradation of Parabens Mediated by Cell Surface Displayed Cutinase

Baotong Zhu and Na Wei*

Department of Civil and Environmental Engineering and Earth Sciences, University of Notre Dame, 156 Fitzpatrick Hall, Notre Dame, Indiana 46556, United States

Supporting Information

ABSTRACT: Parabens are emerging environmental contaminants with known endocrine-disrupting effects. This study created a novel biocatalyst (named as SDFsC) by expressing the enzyme *Fusarium solani pisi* cutinase (FsC) on the cell surface of Baker's yeast *Saccharomycese cerevisiae* and demonstrated successful enzyme-mediated removal of parabens for the first time. Parabens with different side chain structures had different degradation rates by the SDFsC. The SDFsC preferentially degraded the parabens with relatively long alkyl or aromatic side chains. The structure-dependent degradability was in a good agreement with the binding energy between the active site of FsC and different parabens. In real wastewater effluent solution, the SDFsC effectively degraded 800 μg/L of propylparaben, butylparaben, and benzylparaben, either as a single compound or as a mixture, within 48 h. The estrogenic activity of parabens was considerably reduced as the parent parabens were degraded into 4-hydroxybenzoic acid via hydrolysis pathway by the SDFsC. The SDFsC showed superior reusability and maintained 93% of its initial catalytic activity after six rounds of paraben degradation reaction. Results from this study provide scientific basis for developing biocatalysis as a green chemistry alternative for advanced treatment of parabens in sustainable water reclamation.

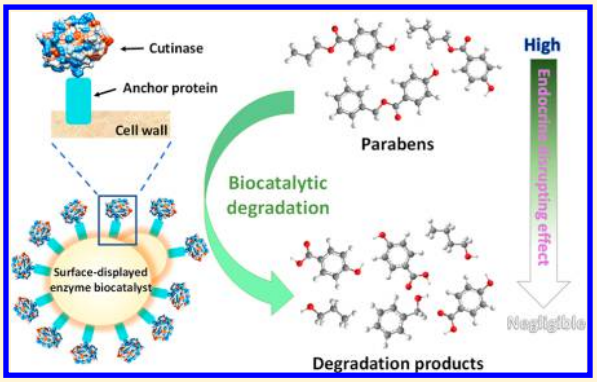

1. INTRODUCTION

Parabens, the esters of para-hydroxybenzoic acid with alkyl or aryl groups substituted as their side chains, are one category of contaminants of emerging concerns due to their ubiquity in the environment and potential health risks.[1,2] Parabens are extensively used as preservative agents in cosmetics, pharmaceuticals, and food products due to their antibacterial and antifungal activity in a wide range of pH.[3−5] The widespread use of parabens and inappropriate disposal have led to their frequent occurrence in the natural and engineered environments,[6−9] and accumulation in aquatic organisms through food webs.[10,11] There is an increasing concern about the risks of parabens on human and other animals because of their endocrine-disrupting effects.[12,13] Numerous in vivo or in vitro toxicology research has reported that parabens exhibit both estrogenic and antiandrogenic activities via binding to the estrogen or androgen receptors, which could result in reproductive disorders and fertilization incapability of the organisms.[14−17]

There is a critical need to develop innovative technologies to effectively and efficiently treat parabens in wastewater reclamation. Wastewater treatment plants are identified as the main channel for emerging contaminants such as parabens to enter the environment because conventional wastewater treatment processes are not designed to eliminate these contaminants. Parabens are frequently detected in secondary wastewater effluents at the concentration level up to micrograms per liter.[2,18] Advanced treatment options for parabens have been extensively investigated in recent years, particularly with a focus on advanced oxidation processes (AOPs) such as H_2O_2/UV system, ozone oxidation, photoassisted Fenton reaction, and heterogeneous photocatalysis.[19−22] However, the high energy input required for UV illumination, expensive chemical reagents, and generation of unknown or more toxic byproducts in AOPs might impede their wide applications in practice.[23,24] Therefore, developing more effective, economical and environmentally sustainable advanced treatment alternatives is critically needed for removing parabens in water reclamation.

Biocatalysis, which uses biological enzymes to catalyze beneficial chemical transformations, has received increasing attention as an emerging green chemistry alternative for degradation of environmental contaminants[25−29] Compared with the AOPs, biocatalysis can perform under ambient conditions with low energy consumption and generate little hazardous byproducts.[29,30] Several classes of enzymes, such as oxidoreductases, hydrolases, and lyases, have demonstrated their applicability in catalyzing the degradation of recalcitrant organic pollutants.[30,31] Parabens can be potentially degraded through

Received: September 18, 2018
Revised: November 21, 2018
Accepted: December 3, 2018
Published: December 3, 2018

DOI: 10.1021/acs.est.8b05275
Environ. Sci. Technol. 2019, 53, 354−364

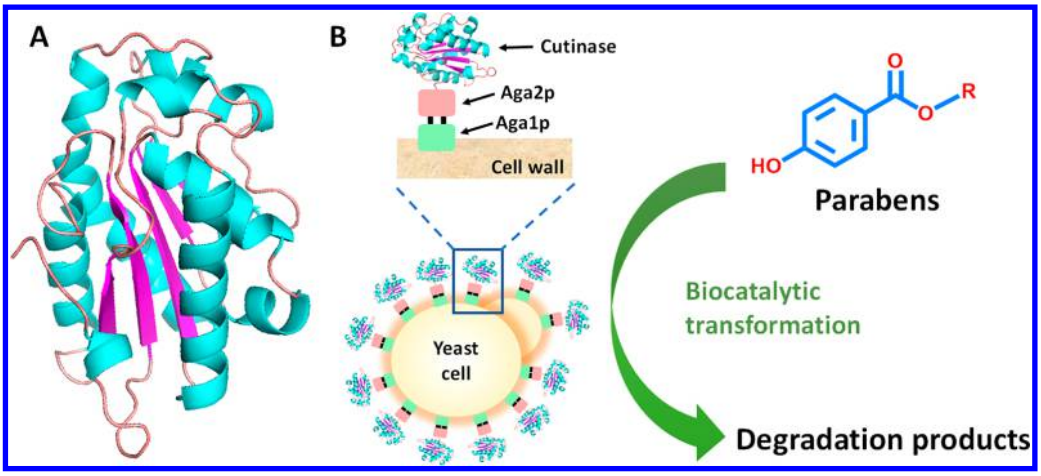

Figure 1. Overview of the design of cell surface-displayed cutinase for biocatalytic degradation of parabens. (A) The 3D structure of the *Fusarium solani pisi* cutinase (FsC). (B) The schematic diagram of the surface-displayed FsC. The FsC is fused with Aga2p subunit of the cell wall protein a-agglutinin which is covalently linked to Aga1p subunit through two disulfide bonds.

enzymatic cleavage of their ester bond by a proper hydrolase. Cutinase (EC 3.1.1.74), originally found in phytopathogenic fungi that can hydrolyze plant cutin polymer,[32] is one promising candidate of such hydrolases. Cutinase can catalytically degrade high-molecular-weight synthetic polyesters, low-molecular-weight soluble esters, and short- and long-chain triacylglycerols.[33] Previous studies have reported that cutinases were capable of degrading some emerging contaminants such as phthalates,[34,35] malathion,[36] and polyester plastics.[37] However, the role of cutinase in enzymatic treatment of environmental pollutants is still underexplored and its potential in paraben degradation has not been reported in existing literature so far.

This study aimed to develop a renewable biocatalyst that harnesses the hydrolytic activity of cutinase for enzymatic removal of parabens in water. Since cutinase can catalyze the hydrolysis of ester bonds, we hypothesized that this enzyme could mediate the paraben degradation. Using enzyme biocatalysts for cost-effective applications generally requires enzyme immobilization to enhance stability and reusability.[38] The conventional ways of enzyme immobilization include covalent binding of enzymes to solid carriers, cross-linking of enzyme aggregates, and entrapment or encapsulation of enzymes within polymeric matrices.[39] However, the chemical reagents used in these methods could denature the enzyme, leading to the loss of enzyme functionality. Additionally, there is still need for time-consuming enzyme purification and preparation.[39] An innovative strategy for enzyme immobilization known as cell surface display has been developed to overcome the above-mentioned drawbacks.[40] The cell surface display technique exploits synthetic biology to engineer renewable biocatalysts by expressing the target enzymes on microbial cell surface.[41] Enzyme functionality and activity can be greatly retained in the cell surface display system while stability and reusability are enhanced as the enzyme is essentially immobilized on the supporting cells. Moreover, this technique circumvents the laborious and costly processes of enzyme isolation and purification because the target enzyme is synthesized intracellularly and then automatically localized on the microbial cell surface through engineered biological machinery.[42] The cell surface display techniques have been applied in the development of biosensors for organic pollutant detection and whole cell biocatalysts for renewable biofuel production.[43−46] Our recent study showed a proof-of-concept demonstration that cell surface display could be used to develop functional, stable, reusable and regenerable biocatalysts for contaminant degradation in water reclamation.[47] Therefore, we exploited the cell surface display platform technology to construct a novel cutinase biocatalyst for degradation of parabens (Figure 1).

In this study, we constructed a new enzyme biocatalyst by expressing the *Fusarium solani pisi* cutinase (FsC) on the cell surface of the Baker's yeast *Saccharomyces cerevisiae* and demonstrated the biocatalytic approach to remove parabens for the first time. We investigated the degradation of various parabens with different side chains by the surface-displayed *F. solani pisi* cutinase (SDFsC) and observed structure-dependent degradability. Molecular docking analysis revealed that the structure-degradability relationships could be explained by the binding interactions of different parabens with FsC. Degradation of parabens by SDFsC substantially reduced estrogenic activity. Analysis of the degradation products confirmed that degradation occurred through hydrolysis of the ester bond. Additionally, the SDFsC could effectively remove single paraben or mixture of parabens in both buffer solution and secondary wastewater effluent. Results from this study provide scientific basis for developing biocatalysis as an innovative advanced treatment alternative to remove parabens and reduce their estrogenic activity in water reclamation.

2. MATERIALS AND METHODS

2.1. Chemicals and Reagents. The structure and physicochemical property of parabens used in this study are summarized in Supporting Information (SI) Table S1. Methyl 4-hydroxybenzoate (methylparaben, MePB), ethyl 4-hydroxybenzoate (ethylparaben, EtPB), propyl 4-hydroxybenzoate (propylparaben, PrPB), butyl 4-hydroxybenzoate (butylparaben, BuPB), benzyl 4-hydroxybenzoate (benzylparaben, BzPB), and 4-hydroxybenzoic acid (4-HbA) were purchased from Sigma-Aldrich (St. Louis, MO). Methyl 3-chloro-4-hydroxybenzoate (monochlorinated methylparaben, Cl−MePB) and *iso*-propyl 4-hydroxybenzoate (*iso*-propylparaben, *i*-PrPB) were purchased from Alfa Aesar (Tewksbury, MA) and TCI (Tokyo, Japan), respectively. The purity for all parabens is higher than 98%. HEPES buffer, *para*-nitrophenyl acetate (pNPA), *para*-nitrophenyl butyrate (pNPB), D-(+)-galactose, bovine serum albumin (BSA), and 17β-estradiol were supplied by Sigma-

DOI: 10.1021/acs.est.8b05275
Environ. Sci. Technol. 2019, 53, 354−364

Aldrich (St. Louis, MO). Restriction enzymes, ligase, and reagents for cloning work were obtained from New England Biolabs (Beverly, MA).

2.2. Strains and Medium. *S. cerevisiae* EBY100 strain (MATa *ura* 3−52 *trp* 1 *leu*2Δ1 *his*3Δ200 *pep*4:*HIS*3 *prb*1Δ1.6R *can*1 *GAL*) (ATCC, Manassas, VA) was used as the host strain for surface display system. *Escherichia coli* TOP10 strain was used for recombinant DNA cloning and manipulation. Recombinant *E. coli* TOP10 was cultured in Luria−Bertani (LB) medium supplemented with 100 mg/L ampicillin. *S. cerevisiae* strains were cultivated in yeast peptone dextrose (YPD) medium or synthetic complete medium without tryptophan (SC-Trp).

2.3. Construction and Preparation of SDFsC Biocatalyst. The microbial strains and plasmids in this study are listed in SI Table S2. The *CUT1* gene encoding the cutinase from a fungal plant pathogen, *F. solani pisi*, was codon-optimized for functional expression in *S. cerevisiae* and synthesized by Genscript (Piscataway, NJ). The signal peptide and stop codon of the *CUT1* were excluded. The *CUT1* was cloned into the pCTcon2 plasmid backbone with *Nhe*I and *Bam*HI restriction enzyme sites at the 5′ and 3′ ends, respectively (SI Figure S1A). The plasmid was transformed into *E. coli* TOP10 competent cells, followed by screening on LB agar plates with 100 mg/L ampicillin. Plasmid extraction from *E. coli* TOP10 cells was then conducted using the QIAprep Spin Miniprep Kit (QIAGEN Inc., Germantown, MD). The resulting recombinant plasmid was confirmed using Sanger sequencing and named as pCTcon2-FsC (SI Figure S1B). Transformation of pCTcon2-FsC into *S. cerevisiae* EBY100 strain was performed using the LiAc/PEG method.[48] The control strain was constructed by transformation of empty pCTcon2 without *CUT1* gene into *S. cerevisiae* EBY100. Yeast transformants harboring pCTcon2-FsC were selected on SC-Trp agar plates and single colonies were isolated to obtain as the SDFsC biocatalyst.

To prepare active SDFsC biocatalyst, the yeast cells harboring pCTcon2-FsC were first cultured in SC-Trp liquid medium for ∼30 h to reach their early stationary growth phase. Then, the cells were pelleted by centrifugation and inoculated into fresh SC-Trp medium supplemented with 20 g/L D-(+)-galactose and 2 g/L dextrose and grown in flasks at 260 rpm and 30 °C to induce expression of the target enzyme. After ∼18 h cultivation (when OD_{600} = 3−4), the induced cells were harvested by centrifugation and washed three times using 10 mM HEPES buffer (pH 7). Yeast cells with pCTcon2 backbone as negative control cells were grown and induced in parallel.

2.4. Enzyme Activity Assay. The enzyme activity of the SDFsC was determined by colorimetrically measuring the hydrolysis rate of *para*-nitrophenyl ester using a method adapted from a previous study.[49] Briefly, 20 μL of SDFsC was added to 180 μL of 10 mM HEPES buffer (pH 7) containing 5 mM pNPA and 10% DMSO. The increase of absorbance at 405 nm due to the hydrolytic release of *para*-nitrophenol (ε 405 nm = 6225 M^{-1} cm^{-1}) was monitored every 2 min for 30 min at 30 °C under continuous shaking condition in a Synergy HT microplate reader (BioTek, Winooski, VT). A blank control was set up by adding all the reagents except SDFsC, and the background hydrolysis rate of pNPA obtained from blank control was subtracted from each assay. The enzyme activity was calculated and expressed in units (U), where 1 U is defined as the amount of enzyme required to catalyze 1 μmol of substrate per minute under the given assay conditions. All measurements were performed in triplicates.

2.5. Immunofluorescence Assay. The immunofluorescence assay was performed to determine the functional expression and appropriate localization of cutinase. The method was slightly modified from previously published protocols,[50,51] and described in detail in the SI.

2.6. Paraben Degradation Experiments. The paraben degradation experiments using SDFsC as the biocatalyst were performed in 14 mL test tubes at 30 °C with 260 rpm shaking. Each tube contained 5 mL of 10 mM HEPES buffer (pH 7) with 10 mg/L each kind of paraben and 0.2 U/mL SDFsC. At predetermined time intervals, aliquots of solution were sampled and immediately centrifuged to separate the SDFsC from solution, and the supernatants were collected for quantifying paraben concentration. Negative control experiments were also conducted in parallel using yeast cells harboring the empty pCTcon2 plasmid without surface display of FsC. Reactions with no yeast cells was set up as abiotic control. Triplicates were conducted for all experiments.

Degradation experiments in actual wastewater effluent with low concentrations of parabens were also performed. The wastewater effluent samples were collected from the outlet of secondary clarifier from the municipal wastewater treatment plant in South Bend, IN. The detailed characteristics of the effluent sample were listed in SI Table S3. The effluent was filtered through a 0.2 μm poly(ether sulfone) membrane, and its pH was adjusted to 7.0. The degradation experiments were performed in 14 mL test tubes containing 5 mL of wastewater effluent with either single or mixture of parabens. The concentration of each paraben in single or mixture for degradation was chosen as 800 μg/L to mimic the environmentally relevant real-world scenario.[2,18] The working enzyme activity of SDFsC added was 0.2 U/mL, which was consistent with that in the degradation experiments in HEPES buffer. Abiotic and negative controls were included, and all experiments were conducted in triplicate.

Kinetic studies were performed for analyzing the degradation process of parabens and the reactions were found to fit the pseudo-first order kinetics.[52]

$$-\frac{dC}{dt} = kC \quad (1)$$

(1)Where k is the pseudo-first order reaction rate coefficient and C is the paraben concentration at time t.

2.7. Molecular Docking. Molecular docking was conducted to simulate the binding modes of each paraben to FsC using Autodock 4.2.[53] The 3D crystal structures of FsC (PDB ID: 1OXM) was obtained from RCSB (Research Collaboratory for Structural Bioinformatics) Protein Data Bank (http://www.rcsb.org/pdb) and then refined by the removal of the ligand and water molecules, addition of missing hydrogens and computation of Gasteiger charges. The structural models of parabens were generated by ChemDraw 16.0 and the energy minimization was performed using the molecular mechanics method (MM2). Then, rotations and torsions for parabens as the ligands were automatically set in the Autodock Tools (ADT). A 3D affinity grid of 40 × 40 × 40 Å centered around the binding active site cavity of FsC with 0.375 Å space between grid points. The Lamarckian genetic algorithm (LGA) was employed for determining the binding of parabens with FsC. Other docking parameters were set to defaults, including a medium number of 2.5 million energy evaluations, a population size of 150, a maximum of 2700 generations, a mutation rate of 0.02, and

DOI: 10.1021/acs.est.8b05275
Environ. Sci. Technol. 2019, 53, 354−364

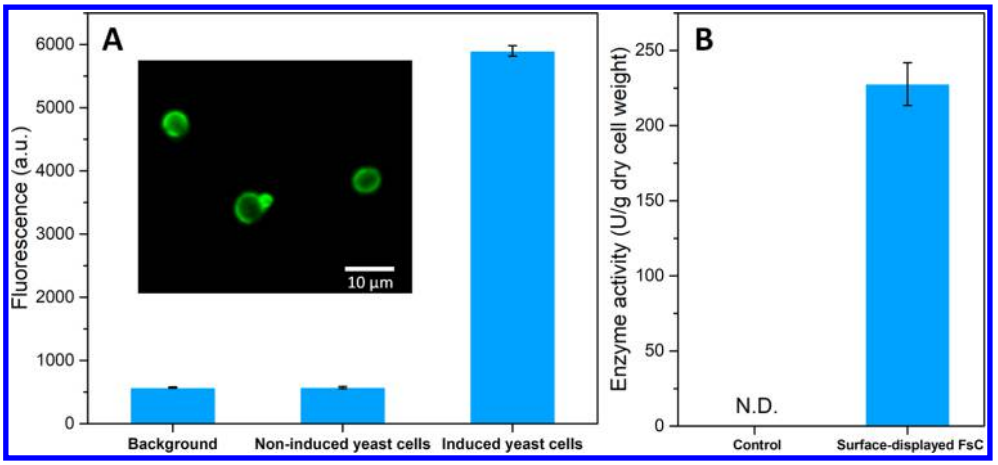

Figure 2. Surface display of functional FsC on yeast cells. (A) Fluorescence intensity of SDFsC cells before and after induction. Inset: Fluorescence microscopy of induced cells with SDFsC labeled with fluorescent antibody. (B) Enzyme activity of SDFsC normalized to the dry cell weight of yeast cells. N.D. denotes not detectable. The experiments were conducted in triplicates and values represent the mean ± standard error.

crossover rate of 0.8. For each simulation, at least 10 independent docking runs were performed.

2.8. Estrogenic Activity Assessment. The estrogenic activity of parabens and their degradation products were determined using a recombinant yeast two-hybrid estrogen screening (rYES) assay as previously described.[54] Specifically, the *S. cerevisiae* W303α with the deletion of the pleiotropic drug resistance gene (*PDR5*) was cotransformed with pG/ER and pUCΔSS-ERE plasmids for the expression of the human estrogen receptor α (ERα) and estrogen-inducible β-galactosidase reporter, respectively. The strain was cultivated in the SC-Trp-Ura medium at 30 °C with shaking at 260 rpm overnight. Then, the yeast cells were collected and grown in fresh SC-Trp-Ura medium with an initial OD_{600} of 0.08 at 30 °C with shaking at 260 rpm. After the OD_{600} reached 0.1, the yeast cells were harvested by centrifugation and subsequently exposed to the parent paraben or the degradation solutions at 30 °C with shaking at 260 rpm for 2 h. Then, 100 μL of the exposed culture was mixed with 100 μL of Gal-screen in Buffer B (Applied Biosystems Inc., Foster City, CA) in an opaque 96-well microplate and incubated at room temperature for another 2 h. The chemiluminescence produced by the activity of β-galactosidase was quantified by the Synergy HT microplate reader. The 17β-estradiol was included as a positive control. All the assays were performed in triplicates.

2.9. Analytical and Instrumental Methods. Quantification of paraben concentration was performed by using a high-performance liquid chromatography system (Waters Alliance 2690, Milford, MA) equipped with a 2996 photodiode array (PDA) detector using an Eclipse XDB-C18 column (Agilent Technologies, Santa Clara, CA). A mixture of methanol and water (v/v = 60:40) was used as the mobile phase with a flow rate of 1 mL/min at 25 °C. The analytes were detected by the PDA detector at the wavelength of 260 nm.

Analysis of the paraben degradation products was carried out by using a Dionex Ultimate 3000 Rapid Separation ultra-performance liquid chromatography (UPLC) system equipped with a Dionex Ultimate 3000 PDA coupled with a Bruker MicrOTOF-Q II quadrupole time-of-flight hybrid mass spectrometer. Chromatographic separations were performed on a Dionex Acclaim RSLC 120 C18 column (2.2 μm, 120 Å, 2.1 mm i.d. × 100 mm) at 40 °C with flow rate of 0.4 mL/min. The mobile phase (A = 0.1% formic acid in water; B = 0.1% formic acid in acetonitrile) gradient consisted of 95% A/5% B for 2 min, followed by a 11 min linear gradient to 0% A/100% B, an 0.1 min linear gradient to 95% A/5% B, and then 95% A/5% B for 1.9 min. The Bruker electrospray ionization source was operated in the negative ion mode with the following parameters: end plate offset voltage = −500 V, capillary voltage = 2200 V, and nitrogen as both a nebulizer (5 bar) and dry gas (10.0 L/min flow rate at 220 °C temperature). Mass spectra were accumulated over the mass range 100−1600 Da at an acquisition rate of 5000 per second.

3. RESULTS AND DISCUSSION

3.1. Functional Display of FsC on Yeast Cell Surface. The surface display of FsC is built on the yeast a-agglutinin system that consists of Aga1p and Aga2p protein subunits (SI Figure S1C). These proteins possess an N-terminal secretion signal sequence for localizing to the cell surface and a C-terminal glycosylphosphatidylinositol (GPI) attachment sequence for anchoring to cell wall.[55] The gene expression cassette in the recombinant plasmid contained the *CUT1* gene encoding the FsC, and two downstream genes encoding the human influenza hemagglutinin (HA) epitope tag and Aga2p respctively and was regulated by the *GAL1* promoter (SI Figure S1B). Upon induction by galactose, the *CUT1* fused with HA epitope tag and Aga2p is expressed, and the N-terminal secretion signal sequence of the Aga2p would subsequently guide the fusion protein to transport outside the cell. Finally, the fusion protein would be automatically immobilized on the yeast cell surface through two disulfide bonds covalently linking the Aga2p to the Aga1p which is attached to the cell wall via the GPI anchor (SI Figure S1C).

The correct surface display of FsC on the yeast cells was confirmed by immunofluorescence labeling technique. The HA epitope tag can bind to the primary anti-HA tag antibody, followed by the binding to the secondary FITC-conjugated antibody with green fluorescence. The SDFsC after induction and labeling exhibited green fluorescence on the cell surface when observed under fluorescence microscope, and it also showed strong fluorescence intensity (Figure 2A). In contrast, the fluorescence intensity of noninduced SDFsC was the same as the background signal of the PBS buffer negative control. Additionally, the enzyme activity of SDFsC was quantified by measuring the hydrolysis rate of pNPA, a model substrate

DOI: 10.1021/acs.est.8b05275
Environ. Sci. Technol. 2019, 53, 354−364

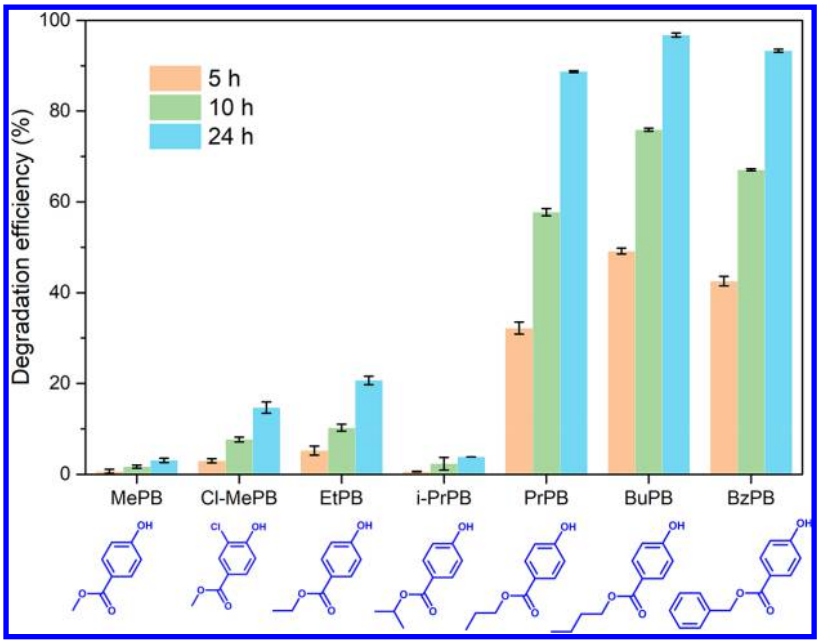

Figure 3. Degradation efficiencies of different parabens by the SDFsC. The initial paraben concentration was 10 mg/L. Experiments were conducted in HEPES buffer (pH 7) with 0.2 U/mL SDFsC. The experiments were conducted in triplicates and values represent the mean ± standard error.

commonly used for hydrolase activity assay.[56,57] The SDFsC had the enzyme activity of 228 ± 14 U/g dry cell weight, whereas there was no detectable activity for control yeast cells harboring empty pCTcon2 after induction (Figure 2B). These results demonstrated that functional FsC was successfully expressed on the yeast cell surface.

We further characterized the fundamental enzyme kinetic properties of the SDFsC biocatalyst using the Michaelis–Menten model:

$$V = V_{max}[S]/(K_m + [S]) \quad (2)$$

where V is the initial reaction rate, V_{max} is the maximum reaction rate at saturating substrate concentration, $[S]$ represents the substrate concentration, K_m is the Michaelis–Menten constant, representing the substrate concentration at which the reaction rate reaches to 50% of V_{max}. The assays were performed under the same reaction condition as the enzyme activity test using two common *p*-nitrophenyl ester substrates for cutinase, pNPA and pNPB, at the concentration ranging from 200 to 8000 μM and from 100 to 3000 μM, respectively.

The enzyme kinetics for SDFsC fitted the Michaelis–Menten model (SI Figure S2). The K_m values of the SDFsC for pNPA and pNPB were 3.1 ± 0.5 mM and 0.67 ± 0.15 mM, respectively, which are well consistent with the values tested using the isolated and purified free FsC reported in previous research (3.0 ± 0.7 mM and 0.47 ± 0.03 mM for the pNPA and pNPB, respectively),[58] indicating that surface display of FsC did not substantially influence the interactions between the substrates and enzyme. The observation was in agreement with prior reports regarding the advantage of the cell surface display strategy compared to conventional enzyme immobilization approaches: enzyme cell surface display could reduce mass transfer limitations because the enzyme is exposed to external environment and could directly interact with the substrate.[40,59] The data suggest that the SDFsC has greater affinity toward pNPB than pNPA. The V_{max} for pNPB was almost twice as much as that for pNPA (SI Figure S2), which means that the SDFsC could catalyze the conversion of pNPB at a faster rate than that of pNPA. The enzyme kinetics data indicate that the hydrolytic activity of SDFsC for the p-nitrophenyl ester with longer chain length (e.g., four carbon atoms in pNPB) would be higher than the one with shorter chain length (e.g., two carbon atoms in pNPA). Similarly, it was reported that when using purified FsC to hydrolyze triglyceride analogues, the enzyme activity increased as the acyl chain length increased from 1 to 4 carbon atoms.[60]

3.2. Structure-Dependent Degradability of Parabens by SDFsC. Considering that the substrate structure variations might affect the degradation activity, we chose a series of commonly used parabens with different side chain structures (SI Table S1) to access their degradation by SDFsC. They include parabens with an alkyl side chain of varied lengths (e.g., MePB, EtPB, *i*-PrPB, PrPB, and BuPB) and one with an aromatic side chain, BzPB, all of which have been widely found in both municipal sewage and natural water environments.[2,8] In addition, a chlorinated paraben, Cl–MePB, was also included since it is a chlorinated derivative commonly generated during the disinfection process in wastewater treatment. It was found that chlorinated paraben byproducts were more toxic and recalcitrant than their parent compounds.[6,61,62] The degradation experiment results showed that only ~3% of MePB was degraded by the SDFsC after 24 h, but the degradation efficiency of EtPB was substantially higher (~20%) though still at a relatively low level (Figure 3). In a sharp contrast, the SDFsC could effectively degrade PrPB and BuPB with an efficiency of 89% and 97%, respectively after 24 h. In comparison, it was reported that the UVC or UVC/H_2O_2 system removed ~50%–60% of PrPB and BuPB in previous research,[63,64] suggesting the high efficacy of SDFsC in treating these two kinds of parabens. Besides, as for the paraben with an aromatic side chain BzPB, the degradation efficiency was 93% at 24 h, suggesting that the SDFsC can also effectively degrade this kind of paraben. No degradation was observed for all the parabens by the control yeast cells without expressing FsC on their surface (SI Figure S3). A small amount of adsorption might contribute to the paraben concentration decrease in the

DOI: 10.1021/acs.est.8b05275
Environ. Sci. Technol. 2019, 53, 354–364

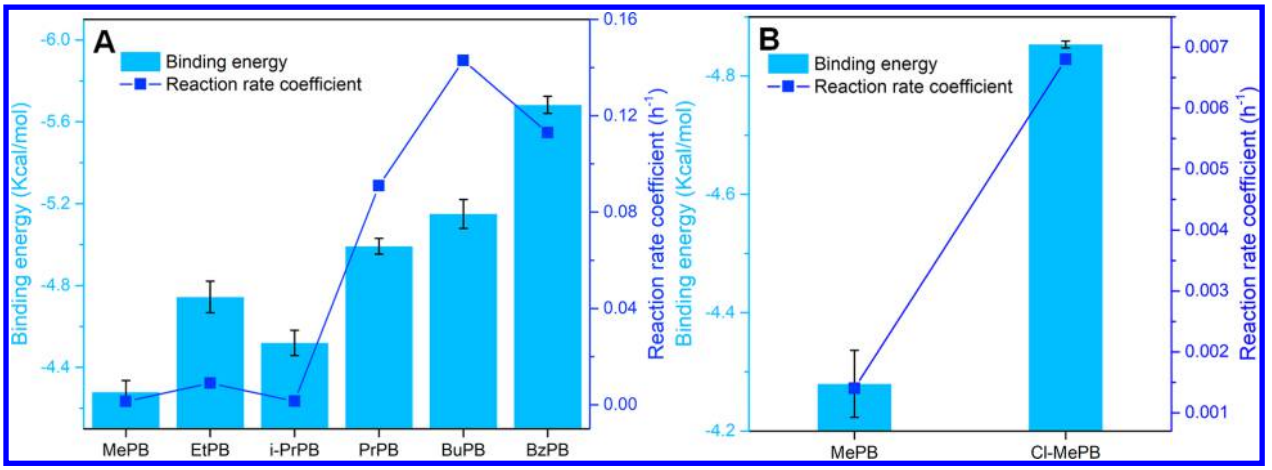

Figure 4. Correlation of binding energy between FsC and parabens with the degradation kinetics of parabens. (A) Parabens with different alkyl or aromatic side chains. (B) Parent MePB and its chlorinated derivative Cl−MePB.

experiments with control cells: 0.8% for MePB, 1.7% for Cl−MePB, 2.4% for EtPB, 2.9% for *i*-PrPB, 8.5% for PrPB, 13.8% for BuPB, and 18.2% for BzPB. Also, the paraben degradation by the SDFsC was further investigated by analyzing the reaction kinetics using linear regression method. According to the kinetic parameters in SI Figure S4 and Table S4, the degradation of all parabens followed the pseudo-first order reaction, similar to the observation when using AOPs to remove parabens.[19,52] The reaction rate coefficients were 0.0013 h^{-1}, 0.009 h^{-1}, 0.092 h^{-1}, and 0.143 h^{-1} for MePB, EtPB, PrPB, and BuPB, respectively, increasing with their alkyl side chain length. These results suggest that the parabens with relatively long alkyl side chain (e.g., PrPB and BuPB) would be preferentially degraded by the SDFsC compared to the ones with relatively short alkyl side chain (e.g., MePB and EtPB). Currently, no existing research data are available on the cutinase-mediated paraben degradation, but a study characterizing an esterase from *Aspergillus oryzae* also reported an elevated enzyme activity toward parabens as their alkyl side chain length increased.[65]

Additionally, the Cl−MePB exhibited improved degradation efficiency compared to its parent compound MePB (SI Figure S3A and B), with a reaction rate coefficient five times higher than that of MePB (SI Figure S4 and Table S4). Chlorinated parabens are normally found to be more recalcitrant than their parent compounds in ozonation processes,[6] but our data indicated that biocatalysis by the SDFsC would favor the degradation of chlorinated parabens. The results suggest that biocatalysis could be a promising treatment alternative to degrade chlorinated parabens and future work to this end is worthwhile to pursue. Notably, the SDFsC also showed stereoselectivity to the paraben isomers PrPB and *i*-PrPB. Nearly 90% of PrPB was degraded after 24 h. whereas only 4% of *i*-PrPB was removed (Figure 3A and SI Figure S3D), which could be due to that the paraben isomers have different interactions with the FsC active site. In summary, the results demonstrate that the degradability of different parabens by the SDFsC is structure-dependent.

3.3. Molecular Interactions of FsC with Parabens. To gain further insights into the structure-dependent degradability of parabens by the SDFsC, molecular docking analysis was performed to investigate the molecular interactions between FsC and different parabens. Molecular docking is a useful tool for simulating and predicting the interaction of an enzyme of interest with the substrate molecule in biocatalysis.[66−68] The 3D crystal structure of FsC is shown in SI Figure S5, and the paraben molecules were docked into its catalytic active site cavity. FsC has a classic catalytic triad as its active site, which consists of SER120, ASP175, and HIS188, and it also has an oxyanion hole that comprises two main-chain nitrogen atoms from SER42 and GLN121.[69−71] In the enzyme biocatalysis, the oxyanion hole plays a crucial role in stabilizing the transition state of the substrate and lowering the activation energy, which facilitates the reaction.[32] Binding of the substrate carbonyl group with the oxyanion hole is essential for initiating the reaction catalyzed by FsC.[69] When the carbonyl group is held in the place of oxyanion hole composed of SER42 and GLN121, it will undergo a nucleophilic attack from the side chain oxygen of SER120 which is deprotonated by the proton shuttle HIS188, and this serves as the starting step for the enzyme biocatalysis.[71] Therefore, a structure is considered to be correctly docked for catalytic reaction if the carbonyl headgroup of parabens interacts with the oxyanion hole and is also within the appropriate distance (1.5−3.0 Å) to SER120 hydroxyl group for nucleophilic attack.[72]

The representative binding complexes between FsC and various parabens are illustrated in SI Figure S6. According to these docked structures, the carbonyl oxygen of all parabens formed two hydrogen bonds with the peptidic amine groups of SER42 and GLN12, respectively. Meanwhile, their carbonyl carbon was at an ideal catalytic distance from SER120 (2.6−2.9 Å). Also, these modeled molecular interactions are similar to the crystallographic binding patterns between FsC and other substrates in previous studies,[71,73] suggesting the accuracy of the docking method used herein. The binding energies for correctly docked complex structures of FsC with different parabens were calculated (Figure 4). The binding energy values for parabens with different alkyl side chains were: MePB (−4.28 kcal/mol) < i-PrPB (−4.52 kcal/mol) < EtPB (−4.74 kcal/mol) < PrPB (−5.00 kcal/mol) < BuPB (−5.15 kcal/mol), indicating that the binding of different parabens with FsC generally became stronger as their side chain size increased. Furthermore, the trend of binding energies for these parabens with different alkyl side chains was in a good agreement with that of their reaction rate coefficients for degradation by SDFsC (Figure 4A). For the BzPB with an aromatic side chain, its binding energy and reaction rate coefficient are both higher than parabens with alkyl side chain except BuPB. A good correlation between the binding energy and reaction rate coefficient was also observed for MePB and its chlorinated derivative, Cl−MePB (Figure 4B). These

DOI: 10.1021/acs.est.8b05275
Environ. Sci. Technol. 2019, 53, 354−364

results showed that the degradability of different parabens generally increased with their binding energy with FsC. Similar trends were also reported for other enzyme−substrate interactions. For example, Arun et al. reported that pyrene with the highest binding interaction with ligninolytic enzymes also showed the maximum degradation efficiency compared with other polycyclic aromatic hydrocarbons.[74] More recently, it was also found that the mutant poly(ethylene terephthalate) (PET) degrading enzyme was capable of hydrolyzing PET more efficiently than the wild-type enzyme, which might be attributed to its higher binding energy with the substrate as modeled by molecular docking.[75] In summary, the structure-dependent degradability for parabens by the SDFsC could result from their different binding abilities with FsC, which directly influences the interaction between paraben and the active site cavity and thus degradation efficiency.

3.4. Estrogenic Activity of Paraben Degradation Products. We quantified the estrogenic activities of parabens and their degradation products to determine how biocatalytic degradation by the SDFsC would reduce the risk of endocrine disrupting effects of the contaminants. The estrogenic activity of 17β-estradiol, a natural estrogen steroid hormone to human ERα, was measured in parallel as a positive control in the rYES assay (SI Figure S7A). Because PrPB, BuPB, and BzPB could be efficiently removed by the SDFsC and they were also previously reported to have stronger estrogenic activity than other paraben analogues,[15] these three parabens were used to evaluate the estrogenic activity during the degradation by the SDFsC. The EC_{50} values for PrPB, BuPB, and BzPB were 2.78×10^{-6}, 1.39×10^{-6}, and 1.26×10^{-6} M, respectively, as determined by their dose−response curves (SI Figure S7B), which were close to the results reported previously,[76] validating the assay performed herein. Figure 5 shows that the estrogenic activity of each

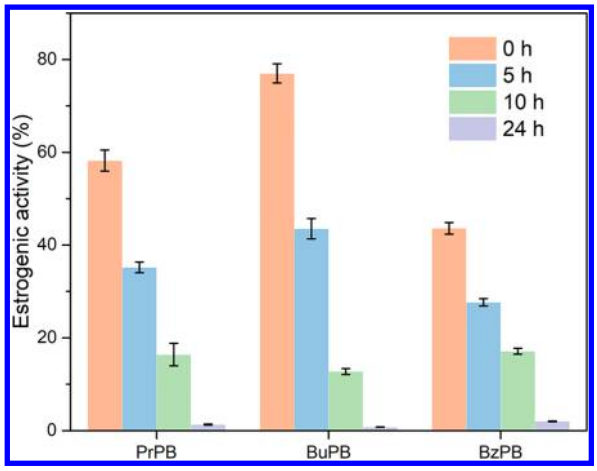

Figure 5. Estrogenic activity during the paraben degradation by the SDFsC. The estrogenic activity is presented as the percentage response normalized by the maximum activity of 17β-estradiol observed at the concentration of 1×10^{-7} M. The experiments were conducted in triplicates and values represent the mean ± standard error.

paraben was significantly reduced along the degradation process and was almost eliminated after 24 h. The results suggest that the degradation catalyzed by the SDFsC could effectively deactivate the estrogenic effects of these parabens. Watanabe et al. also found that the estrogenic activity of BuPB was considerably diminished when treated with rat liver microsomes, probably due to the hydrolytic effect of carboxylesterase.[15]

To better understand the degradation mechanism, we analyzed the degradation products of PrPB, BuPB, and BzPB after 10 h incubation using UPLC coupled with PDA detector and MS. The chromatograms showed that there was a new peak representing the degradation product at the retention time of around 4.2 min besides the parent parabens (at the retention time of 7.4−7.9 min) for all the three parabens (SI Figure S8B−D). This new peak had an identical retention time to the commercial 4-HbA standard (SI Figure S8A). The mass spectrometric fragmentations of the degradation product and 4-HbA standard were shown in SI Figure S9. The precursor ion of the degradation product with the m/z value of 137 Da is the $[M-H]^-$ fragment of the 4-HbA with a molecular weight of 138 Da. Therefore, based on the matched chromatograms and MS spectra, the paraben degradation product could be identified as the 4-HbA. The data indicate that the ester bond of parabens is cleaved by SDFsC via the hydrolysis pathway, yielding 4-HbA and the corresponding alcohols, which have negligible estrogenic activity.[15,77] Besides the endocrine disrupting effect, prior studies have reported that 4-HbA exhibited no significant toxicity to a variety of organisms using both in vivo and in vitro acute or chronic toxicity tests.[78,79] For example, 4-HbA showed no remarkable cytotoxicity in mitochondrial dysfunction toward the rat hepatocytes.[80] Also, no evidence of blood damage or histological changes in mice tissues was observed when treated with 4-HbA through oral, intravenous, and intraperitoneal administration.[81] Collectively, the SDFsC could degrade the harmful parabens into environmentally benign product.

3.5. Paraben Degradation by SDFsC under Environmentally Relevant Conditions. Experiments on the degradability of parabens by the SDFsC in actual wastewater effluent were performed, with the motivation to examine the feasibility of the biocatalytic process as an advanced treatment alternative in water reclamation. Secondary wastewater effluent sample was collected from South Bend Wastewater Treatment Plant. PrPB, BuPB, and BzPB were selected considering their efficient removal by the SDFsC in HEPES buffer solution and relatively high endocrine-disrupting effects as discussed above. It is worth mentioning that the degradation experiments were not only performed for single paraben system but also for mixture of parabens (i.e., mixture of PrPB and BuPB as well as mixture of PrPB and BzPB) because they are frequently used as a blend in personal care products and detected concomitantly in wastewater.[2,3] For comparison, experiments using HEPES buffer under the same incubation conditions were conducted in parallel.

As shown in Figure 6, the SDFsC could effectively degrade the three parabens, whether for the single paraben or their mixtures, in both the HEPES buffer solution and wastewater effluent matrix. More than 98% of PrPB and all of BuPB and BzPB were removed within 48 h incubation, and their degradation profile followed the pseudo-first order kinetics (SI Figure S10). Comparing the degradation kinetics between the wastewater effluent matrix and HEPES buffer, the degradation rate for PrPB was only slightly lower in wastewater effluent than in HEPES buffer, and there was no significant difference (t test, $P > 0.05$) observed for BuPB or BzPB degradation between the two systems (SI Figure S10 and Table S5). The results suggest that the wastewater effluent matrix condition had negligible adverse impacts on the performance of the SDFsC. A previous study on characterizing purified FsC also reported that there was no significant inhibition from some metal ions commonly found in wastewater, such as Mn^{2+}, Co^{2+}, Ni^{2+}, Mg^{2+}, Cu^{2+}, and Ca^{2+}, on

DOI: 10.1021/acs.est.8b05275
Environ. Sci. Technol. 2019, 53, 354−364

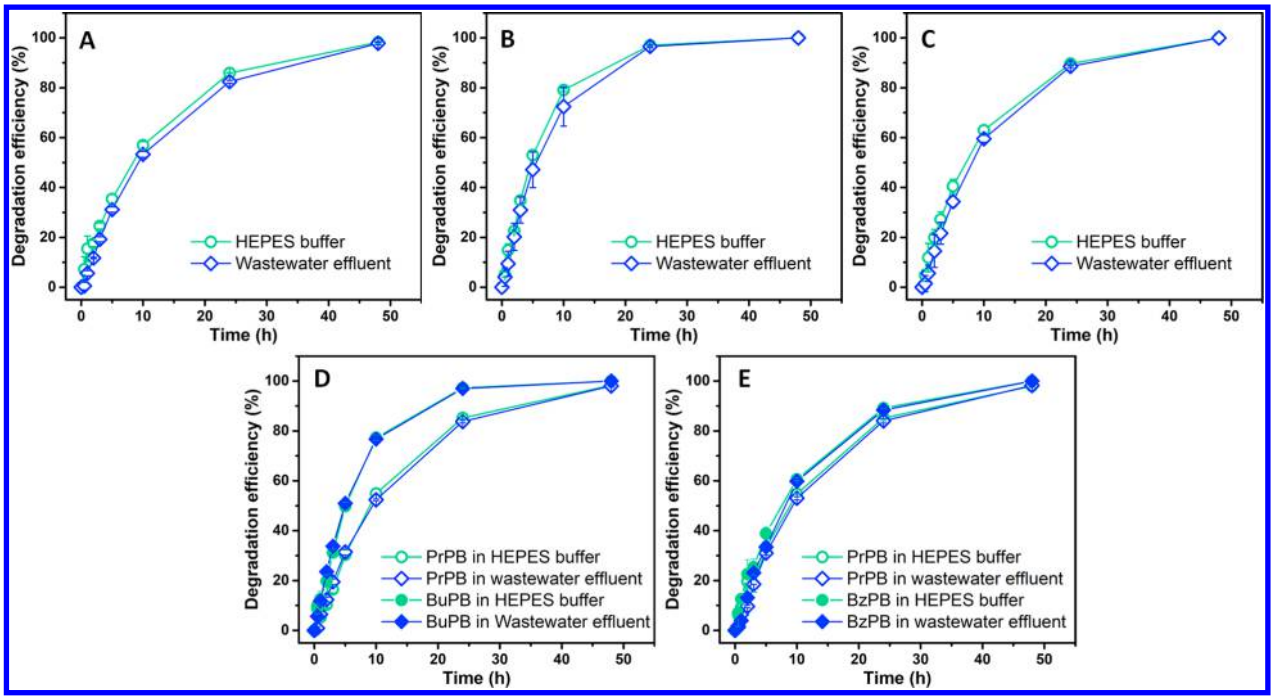

Figure 6. Degradation of parabens by the SDFsC in HEPES buffer and secondary wastewater effluent. The initial paraben concentration was 800 μg/L. Experiments were conducted in HEPES buffer or wastewater effluent at pH 7 with 0.2 U/mL SDFsC. (A) Single PrPB. (B) Single BuPB. (C) Single BzPB. (D) Mixture of PrPB and BuPB. (E) Mixture of PrPB and BzPB. The experiments were conducted in triplicates and values represent the mean ± standard error. Error bars indicating standard deviations are not visible when smaller than the symbol size.

the enzyme activity,[82] and this feature is advantageous when using FsC in wastewater treatment. Furthermore, the SDFsC also exhibited excellent performance in the degradation of paraben mixtures, and the degradation efficiency and kinetics for each paraben in the mixture were almost the same with those in the single compound solution (Figure 6 and SI Figure S10 and Table S5). Research on removal of mixed parabens is quite scarce so far.[19,83] In a previous study using UVC and UVC/H_2O_2 treatment processes, it was found that the degradation for each paraben was retarded in the mixture compared to that in the single compound system.[83] In contrast, the enzymatic degradation of parabens by the SDFsC had similar efficiencies in single and mixture systems, suggesting the capability and feasibility of SDFsC in treating concomitant parabens in wastewater.

An important and desirable feature of the SDFsC for practical application in wastewater treatment lies in its reusability, which would considerably lower the operation cost. The SDFsC, which can be essentially viewed as biocatalytic microparticles with the size of 5−10 μm, will be easily recovered from aqueous solutions by simple filtration, and the collected biocatalyst then can be reused. To determine the reusability of SDFsC, we performed repeated batch experiments for degrading 800 μg/L BuPB with an initial amount of SDFsC equivalent to 0.2 U/mL enzyme activity. At the end of each cycle of the degradation experiment, the SDFsC cells were pelleted by centrifugation, resuspended and washed in HEPES buffer solution. The washing steps were repeated for three times and then the SDFsC cells were used again for the next cycle of experiment. As shown in SI Figure S11, the relative degradation efficiency after six cycles of reaction still retained more than 90% compared to that in the initial cycle. The results demonstrate that the SDFsC has good stability in reuse and such feature would be advantageous in developing cost-effective treatment technology for practical use.

4. ENVIRONMENTAL IMPLICATIONS

This study created a novel biocatalyst based on surface display of a fungal cutinase on yeast cells using synthetic biology and demonstrated successful enzyme-mediated removal of parabens for the first time. The SDFsC could catalyze efficient degradation of parabens and considerably mitigate their endocrine disrupting activity, especially for the ones with relatively long alkyl or aromatic side chains which are of greater concern for their risks to human health and ecosystems.[84] The biocatalytic process is distinct from existing methods (e.g., membrane processes, AOPs) in that it operates at ambient temperature and pressure without need to add other chemical reagents or high energy input, and the SDFsC biocatalyst could be recovered and reused. As demonstrated in this study, the SDFsC biocatalyst could perform well in real-world secondary effluent, which holds great promise for eventually developing an efficient and cost-effective technology as an innovative advanced treatment alternative in water reclamation. The biocatalytic treatment could either operate alone or in combination with other treatment technologies for a polishing step. A recent study on perchlorate treatment also reported that enzyme biocatalysis would be more competitive than existing methods in terms of costs and environmental impacts.[26] Future work will develop a biocatalytic reactor system for continuous processes while retaining the biocatalyst in the system for easy recovery and reuse.

Additionally, it is worth noting that cutinases have a wide range of substrates[33] and hold great promise for enzymatic degradation of various environmental pollutants other than parabens. Cutinase-mediated degradation could be exploited for contaminants which have ester bonds in their structure and have reduced risks after hydrolysis of ester bonds.[85] Examples include recalcitrant polyester and polyamide plastics,[37] fats, oils, and grease (FOG) generated from the waste of kitchen cooking and

DOI: 10.1021/acs.est.8b05275
Environ. Sci. Technol. 2019, 53, 354−364

food processing,[86] and ester plasticizers used in material processing.[87] With the proof-of-concept demonstration of using SDFsC as a novel biocatalyst for parabens, similar biocatalytic treatment processes for a broader array of contaminants as mentioned above could be developed in future work, opening up new opportunities of using enzyme biocatalysis as a green chemistry alternative to address more environmental challenges.

■ ASSOCIATED CONTENT

Supporting Information

The Supporting Information is available free of charge on the ACS Publications website at DOI: 10.1021/acs.est.8b05275.

Method for immunofluorescence assay, structures and physicochemical characteristics of parabens used in this study (Table S1), the yeast strains and plasmids used in this study (Table S2), characteristics of the secondary wastewater effluent sample (Table S3), paraben degradation kinetic parameters (Table S4), degradation kinetics parameters for single and mixed parabens in HEPES and wastewater effluent (Table S5), yeast cell surface display system (Figure S1), Michaelis−Menten kinetics for pNPA and pNPB (Figure S2), paraben degradation by control cells (Figure S3), degradation kinetics of different parabens by the SDFsC (Figure S4), 3D structure of FsC (Figure S5), binding complexes of FsC with parabens (Figure S6), dose−response curves for estrogenic activity tests (Figure S7), chromatograms of degradation products (Figure S8), mass spectrometric fragmentation of degradation product (Figure S9), degradation kinetics for single and mixed parabens in HEPES and wastewater effluent (Figure S10), and reusability of SDFsC (Figure S11) (PDF)

■ AUTHOR INFORMATION

Corresponding Author

*Phone: 574-631-5164; fax: 574-631-9236; e-mail: nwei@nd.edu.

ORCID

Na Wei: 0000-0003-2093-3441

Notes

The authors declare no competing financial interest.

■ ACKNOWLEDGMENTS

This work was supported by National Science Foundation (CBET-1653679). We thank Dr. Mijoon Lee for her assistance in UPLC/MS analysis at the Mass Spectrometry & Proteomics Facility of the University of Notre Dame. We also thank Dr. Robert Nerenberg for his help in fluorescence microscopy. The Center for Environmental Science and Technology of the University of Notre Dame is acknowledged for providing the access to the instrumentation used in this study.

■ ABBREVIATIONS

AOPs	advanced oxidation processes
FsC	*Fusarium solani pisi* cutinase
SDFsC	surface-displayed *F. solani pisi* cutinase
MePB	methylparaben
Cl−MePB	monochlorinated methylparaben
EtPB	ethylparaben
i-PrPB	*iso*-propylparaben
PrPB	propylparaben
BuPB	butylparaben
BzPB	benzylparaben
4-HbA	4-hydroxybenzoic acid
pNPA	*para*-nitrophenyl acetate
pNPB	*para*-nitrophenyl butyrate
rYES	recombinant yeast two-hybrid estrogen screening
UPLC	ultraperformance liquid chromatography

■ REFERENCES

(1) Haman, C.; Dauchy, X.; Rosin, C.; Munoz, J. F. Occurrence, fate and behavior of parabens in aquatic environments: a review. *Water Res.* **2015**, *68*, 1−11.

(2) Bledzka, D.; Gromadzinska, J.; Wasowicz, W. Parabens: From environmental studies to human health. *Environ. Int.* **2014**, *67*, 27−42.

(3) Guo, Y.; Kannan, K. A survey of phthalates and parabens in personal care products from the United States and its implications for human exposure. *Environ. Sci. Technol.* **2013**, *47* (24), 14442−14449.

(4) Liao, C.; Liu, F.; Kannan, K. Occurrence of and dietary exposure to parabens in foodstuffs from the United States. *Environ. Sci. Technol.* **2013**, *47* (8), 3918−3925.

(5) Karthikraj, R.; Borkar, S.; Lee, S.; Kannan, K. Parabens and their metabolites in pet food and urine from New York State, United States. *Environ. Sci. Technol.* **2018**, *52* (6), 3727−3737.

(6) Li, W.; Shi, Y.; Gao, L.; Liu, J.; Cai, Y. Occurrence, fate and risk assessment of parabens and their chlorinated derivatives in an advanced wastewater treatment plant. *J. Hazard. Mater.* **2015**, *300*, 29−38.

(7) Brausch, J. M.; Rand, G. M. A review of personal care products in the aquatic environment: environmental concentrations and toxicity. *Chemosphere* **2011**, *82* (11), 1518−1532.

(8) Bu, Q.; Wang, B.; Huang, J.; Deng, S.; Yu, G. Pharmaceuticals and personal care products in the aquatic environment in China: a review. *J. Hazard. Mater.* **2013**, *262*, 189−211.

(9) Wang, W.; Kannan, K. Fate of parabens and their metabolites in two wastewater treatment plants in New York State, United States. *Environ. Sci. Technol.* **2016**, *50* (3), 1174−1181.

(10) Xue, J.; Sasaki, N.; Elangovan, M.; Diamond, G.; Kannan, K. Elevated accumulation of parabens and their metabolites in marine mammals from the United States coastal waters. *Environ. Sci. Technol.* **2015**, *49* (20), 12071−12079.

(11) Xue, X.; Xue, J.; Liu, W.; Adams, D. H.; Kannan, K. Trophic magnification of parabens and their metabolites in a subtropical marine food web. *Environ. Sci. Technol.* **2017**, *51* (2), 780−789.

(12) Boberg, J.; Taxvig, C.; Christiansen, S.; Hass, U. Possible endocrine disrupting effects of parabens and their metabolites. *Reprod. Toxicol.* **2010**, *30* (2), 301−312.

(13) Darbre, P. D.; Harvey, P. W. Paraben esters: review of recent studies of endocrine toxicity, absorption, esterase and human exposure, and discussion of potential human health risks. *J. Appl. Toxicol.* **2008**, *28* (5), 561−578.

(14) Ding, K.; Kong, X.; Wang, J.; Lu, L.; Zhou, W.; Zhan, T.; Zhang, C.; Zhuang, S. Side chains of parabens modulate antiandrogenic activity: *In vitro* and molecular docking studies. *Environ. Sci. Technol.* **2017**, *51* (11), 6452−6460.

(15) Watanabe, Y.; Kojima, H.; Takeuchi, S.; Uramaru, N.; Ohta, S.; Kitamura, S. Comparative study on transcriptional activity of 17 parabens mediated by estrogen receptor alpha and beta and androgen receptor. *Food Chem. Toxicol.* **2013**, *57*, 227−234.

(16) van Meeuwen, J. A.; van Son, O.; Piersma, A. H.; de Jong, P. C.; van den Berg, M. Aromatase inhibiting and combined estrogenic effects of parabens and estrogenic effects of other additives in cosmetics. *Toxicol. Appl. Pharmacol.* **2008**, *230* (3), 372−382.

(17) Garcia, T.; Schreiber, E.; Kumar, V.; Prasad, R.; Sirvent, J. J.; Domingo, J. L.; Gomez, M. Effects on the reproductive system of young male rats of subcutaneous exposure to n-butylparaben. *Food Chem. Toxicol.* **2017**, *106*, 47−57.

(18) Yang, Y.; Ok, Y. S.; Kim, K. H.; Kwon, E. E.; Tsang, Y. F. Occurrences and removal of pharmaceuticals and personal care

products (PPCPs) in drinking water and water/sewage treatment plants: A review. *Sci. Total Environ.* **2017**, *596*−*597*, 303−320.
(19) Steter, J. R.; Brillas, E.; Sires, I. Solar photoelectro-Fenton treatment of a mixture of parabens spiked into secondary treated wastewater effluent at low input current. *Appl. Catal., B* **2018**, *224*, 410−418.
(20) Petala, A.; Noe, A.; Frontistis, Z.; Drivas, C.; Kennou, S.; Mantzavinos, D.; Kondarides, D. I., Synthesis and characterization of CoOx/BiVO4 photocatalysts for the degradation of propyl paraben. *J. Hazard. Mater.* **2018**. DOI: 10.1016/j.jhazmat.2018.03.008
(21) Fang, H.; Gao, Y.; Li, G.; An, J.; Wong, P. K.; Fu, H.; Yao, S.; Nie, X.; An, T. Advanced oxidation kinetics and mechanism of preservative propylparaben degradation in aqueous suspension of TiO_2 and risk assessment of its degradation products. *Environ. Sci. Technol.* **2013**, *47* (6), 2704−2712.
(22) Tay, K. S.; Abd Rahman, N.; Bin Abas, M. R. Kinetic studies of the degradation of parabens in aqueous solution by ozone oxidation. *Environ. Chem. Lett.* **2010**, *8* (4), 331−337.
(23) Zhang, J.; Sun, B.; Guan, X.; Wang, H.; Bao, H.; Huang, Y.; Qiao, J.; Zhou, G. Ruthenium nanoparticles supported on CeO2 for catalytic permanganate oxidation of butylparaben. *Environ. Sci. Technol.* **2013**, *47* (22), 13011−13019.
(24) Wang, W. L.; Wu, Q. Y.; Huang, N.; Xu, Z. B.; Lee, M. Y.; Hu, H. Y. Potential risks from UV/H_2O_2 oxidation and UV photocatalysis: A review of toxic, assimilable, and sensory-unpleasant transformation products. *Water Res.* **2018**, *141*, 109−125.
(25) Naghdi, M.; Taheran, M.; Brar, S. K.; Kermanshahi-Pour, A.; Verma, M.; Surampalli, R. Y. Removal of pharmaceutical compounds in water and wastewater using fungal oxidoreductase enzymes. *Environ. Pollut.* **2018**, *234*, 190−213.
(26) Hutchison, J. M.; Guest, J. S.; Zilles, J. L. Evaluating the development of biocatalytic technology for the targeted removal of perchlorate from drinking water. *Environ. Sci. Technol.* **2017**, *51* (12), 7178−7186.
(27) Dvorak, P.; Bidmanova, S.; Damborsky, J.; Prokop, Z. Immobilized synthetic pathway for biodegradation of toxic recalcitrant pollutant 1,2,3-trichloropropane. *Environ. Sci. Technol.* **2014**, *48* (12), 6859−6866.
(28) Hutchison, J. M.; Poust, S. K.; Kumar, M.; Cropek, D. M.; Macallister, I. E.; Arnett, C. M.; Zilles, J. L. Perchlorate reduction using free and encapsulated Azospira oryzae enzymes. *Environ. Sci. Technol.* **2013**, *47* (17), 9934−9941.
(29) Alcalde, M.; Ferrer, M.; Plou, F. J.; Ballesteros, A. Environmental biocatalysis: from remediation with enzymes to novel green processes. *Trends Biotechnol.* **2006**, *24* (6), 281−287.
(30) Demarche, P.; Junghanns, C.; Nair, R. R.; Agathos, S. N. Harnessing the power of enzymes for environmental stewardship. *Biotechnol. Adv.* **2012**, *30* (5), 933−953.
(31) Chen, Y.; Gao, P.; Summe, M. J.; Phillip, W. A.; Wei, N. Biocatalytic membranes prepared by inkjet printing functionalized yeast cells onto microfiltration substrates. *J. Membr. Sci.* **2018**, *550*, 91−100.
(32) Chen, S.; Su, L.; Chen, J.; Wu, J. Cutinase: characteristics, preparation, and application. *Biotechnol. Adv.* **2013**, *31* (8), 1754−1767.
(33) Nyyssola, A. Which properties of cutinases are important for applications? *Appl. Microbiol. Biotechnol.* **2015**, *99* (12), 4931−4942.
(34) Kim, Y. H.; Min, J.; Bae, K. D.; Gu, M. B.; Lee, J. Biodegradation of dipropyl phthalate and toxicity of its degradation products: a comparison of *Fusarium oxysporum* f. sp. *pisi* cutinase and *Candida cylindracea* esterase. *Arch. Microbiol.* **2005**, *184* (1), 25−31.
(35) Kim, Y. H.; Lee, J.; Ahn, J. Y.; Gu, M. B.; Moon, S. H. Enhanced degradation of an endocrine-disrupting chemical, butyl benzyl phthalate, by *Fusarium oxysporum* f. sp. *pisi* cutinase. *Appl. Environ. Microbiol.* **2002**, *68* (9), 4684−4688.
(36) Kim, Y. H.; Ahn, J. Y.; Moon, S. H.; Lee, J. Biodegradation and detoxification of organophosphate insecticide, malathion by *Fusarium oxysporum* f. sp. *pisi* cutinase. *Chemosphere* **2005**, *60* (10), 1349−1355.
(37) Ferrario, V.; Pellis, A.; Cespugli, M.; Guebitz, G.; Gardossi, L. Nature inspired solutions for polymers: Will cutinase enzymes make polyesters and polyamides greener? *Catalysts* **2016**, *6* (12), 205.
(38) de Carvalho, C. C. Enzymatic and whole cell catalysis: finding new strategies for old processes. *Biotechnol. Adv.* **2011**, *29* (1), 75−83.
(39) Sheldon, R. A.; van Pelt, S. Enzyme immobilisation in biocatalysis: why, what and how. *Chem. Soc. Rev.* **2013**, *42* (15), 6223−35.
(40) Nakatani, H.; Hori, K. Cell surface protein engineering for high-performance whole-cell catalysts. *Front. Chem. Sci. Eng.* **2017**, *11* (1), 46−57.
(41) Kondo, A.; Ueda, M. Yeast cell-surface display−applications of molecular display. *Appl. Microbiol. Biotechnol.* **2004**, *64* (1), 28−40.
(42) Tanaka, T.; Yamada, R.; Ogino, C.; Kondo, A. Recent developments in yeast cell surface display toward extended applications in biotechnology. *Appl. Microbiol. Biotechnol.* **2012**, *95* (3), 577−591.
(43) Fan, S.; Hou, C.; Liang, B.; Feng, R.; Liu, A. Microbial surface displayed enzymes based biofuel cell utilizing degradation products of lignocellulosic biomass for direct electrical energy. *Bioresour. Technol.* **2015**, *192*, 821−825.
(44) Liu, A.; Feng, R.; Liang, B. Microbial surface displaying formate dehydrogenase and its application in optical detection of formate. *Enzyme Microb. Technol.* **2016**, *91*, 59−65.
(45) Liu, A.; Lang, Q.; Liang, B.; Shi, J. Sensitive detection of maltose and glucose based on dual enzyme-displayed bacteria electrochemical biosensor. *Biosens. Bioelectron.* **2017**, *87*, 25−30.
(46) Liang, B.; Wang, G.; Yan, L.; Ren, H.; Feng, R.; Xiong, Z.; Liu, A. Functional cell surface displaying of acetylcholinesterase for spectrophotometric sensing organophosphate pesticide. *Sens. Actuators, B* **2019**, *279*, 483−489.
(47) Chen, Y.; Stemple, B.; Kumar, M.; Wei, N. Cell surface display fungal laccase as a renewable biocatalyst for degradation of persistent micropollutants bisphenol A and sulfamethoxazole. *Environ. Sci. Technol.* **2016**, *50* (16), 8799−8808.
(48) Gietz, R. D.; Schiestl, R. H. High-efficiency yeast transformation using the LiAc/SS carrier DNA/PEG method. *Nat. Protoc.* **2007**, *2* (1), 31−34.
(49) Yoshida, S.; Hiraga, K.; Takehana, T.; Taniguchi, I.; Yamaji, H.; Maeda, Y.; Toyohara, K.; Miyamoto, K.; Kimura, Y.; Oda, K. A bacterium that degrades and assimilates poly(ethylene terephthalate). *Science* **2016**, *351* (6278), 1196−1199.
(50) Tsai, S. L.; Oh, J.; Singh, S.; Chen, R.; Chen, W. Functional assembly of minicellulosomes on the *Saccharomyces cerevisiae* cell surface for cellulose hydrolysis and ethanol production. *Appl. Environ. Microbiol.* **2009**, *75* (19), 6087−6093.
(51) Baek, S. H.; Kim, S.; Lee, K.; Lee, J. K.; Hahn, J. S. Cellulosic ethanol production by combination of cellulase-displaying yeast cells. *Enzyme Microb. Technol.* **2012**, *51* (6−7), 366−372.
(52) Gomes, J. F.; Leal, I.; Bednarczyk, K.; Gmurek, M.; Stelmachowski, M.; Zaleska-Medynska, A.; Quinta-Ferreira, M. E.; Costa, R.; Quinta-Ferreira, R. M.; Martins, R. C. Detoxification of parabens using UV-A enhanced by noble metals—TiO_2 supported catalysts. *J. Environ. Chem. Eng.* **2017**, *5* (4), 3065−3074.
(53) Morris, G. M.; Huey, R.; Lindstrom, W.; Sanner, M. F.; Belew, R. K.; Goodsell, D. S.; Olson, A. J. AutoDock4 and AutoDockTools4: Automated docking with selective receptor flexibility. *J. Comput. Chem.* **2009**, *30* (16), 2785−2791.
(54) Balsiger, H. A.; de la Torre, R.; Lee, W. Y.; Cox, M. B. A four-hour yeast bioassay for the direct measure of estrogenic activity in wastewater without sample extraction, concentration, or sterilization. *Sci. Total Environ.* **2010**, *408* (6), 1422−1429.
(55) Tanaka, T.; Kondo, A. Cell-surface display of enzymes by the yeast *Saccharomyces cerevisiae* for synthetic biology. *FEMS Yeast Res.* **2015**, *15* (1), 1−9.
(56) Ribitsch, D.; Herrero Acero, E.; Przylucka, A.; Zitzenbacher, S.; Marold, A.; Gamerith, C.; Tscheliessnig, R.; Jungbauer, A.; Rennhofer, H.; Lichtenegger, H.; Amenitsch, H.; Bonazza, K.; Kubicek, C. P.; Druzhinina, I. S.; Guebitz, G. M. Enhanced cutinase-catalyzed

DOI: 10.1021/acs.est.8b05275
Environ. Sci. Technol. 2019, 53, 354−364

hydrolysis of polyethylene terephthalate by covalent fusion to hydrophobins. *Appl. Environ. Microbiol.* **2015**, *81* (11), 3586−3592.
(57) Ping, L. F.; Chen, X. Y.; Yuan, X. L.; Zhang, M.; Chai, Y. J.; Shan, S. D. Application and comparison in biosynthesis and biodegradation by *Fusarium solani* and *Aspergillus fumigatus* cutinases. *Int. J. Biol. Macromol.* **2017**, *104* (Pt A), 1238−1245.
(58) Goncalves, A. M.; Serro, A. P.; Aires-Barros, M. R.; Cabral, J. M. S. Effects of ionic surfactants used in reversed micelles on cutinase activity and stability. *Biochim. Biophys. Acta, Protein Struct. Mol. Enzymol.* **2000**, *1480* (1−2), 92−106.
(59) Sankaran, R.; Show, P. L.; Chang, J.-S. Biodiesel production using immobilized lipase: feasibility and challenges. *Biofuels, Bioprod. Biorefin.* **2016**, *10* (6), 896−916.
(60) Mannesse, M. L. M.; Cox, R. C.; Koops, B. C.; Verheij, H. M.; Dehaas, G. H.; Egmond, M. R.; Vanderhijden, H. T. W. M.; Devlieg, J. Cutinase from *Fusarium Solani pisi* hydrolyzing triglyceride analogs - Effect of acyl-chain length and position in the substrate molecule on activity and enantioselectivity. *Biochemistry* **1995**, *34* (19), 6400−6407.
(61) Terasaki, M.; Makino, M.; Tatarazako, N. Acute toxicity of parabens and their chlorinated by-products with *Daphnia magna* and Vibrio fischeri bioassays. *J. Appl. Toxicol.* **2009**, *29* (3), 242−247.
(62) Canosa, P.; Rodriguez, I.; Rubi, E.; Negreira, N.; Cela, R. Formation of halogenated by-products of parabens in chlorinated water. *Anal. Chim. Acta* **2006**, *575* (1), 106−113.
(63) Daghrir, R.; Dimboukou-Mpira, A.; Seyhi, B.; Drogui, P. Photosonochemical degradation of butyl-paraben: Optimization, toxicity and kinetic studies. *Sci. Total Environ.* **2014**, *490*, 223−234.
(64) Cuerda-Correa, E. M.; Domínguez-Vargas, J. n. R.; Muñoz-Peña, M. J.; González, T. Ultraviolet-photoassisted advanced oxidation of parabens catalyzed by hydrogen peroxide and titanium dioxide. Improving the system. *Ind. Eng. Chem. Res.* **2016**, *55* (18), 5152−5160.
(65) Koseki, T.; Mihara, K.; Murayama, T.; Shiono, Y. A novel *Aspergillus oryzae* esterase that hydrolyzes 4-hydroxybenzoic acid esters. *FEBS Lett.* **2010**, *584* (18), 4032−4036.
(66) Suresh, P. S.; Kumar, A.; Kumar, R.; Singh, V. P. An *in silico* approach to bioremediation: Laccase as a case study. *J. Mol. Graphics Modell.* **2008**, *26* (5), 845−849.
(67) Sridhar, S.; Chinnathambi, V.; Arumugam, P.; Suresh, P. K. *In silico* and *in vitro* physicochemical screening of *Rigidoporus* sp. crude laccase-assisted decolorization of synthetic dyes–Approaches for a cost-effective enzyme-based remediation methodology. *Appl. Biochem. Biotechnol.* **2013**, *169* (3), 911−922.
(68) Silva, M. C.; Torres, J. A.; Castro, A. A.; da Cunha, E. F.; Alves de Oliveira, L. C.; Correa, A. D.; Ramalho, T. C. Combined experimental and theoretical study on the removal of pollutant compounds by peroxidases: affinity and reactivity toward a bioremediation catalyst. *J. Biomol. Struct. Dyn.* **2016**, *34* (9), 1839−1848.
(69) Egmond, M. R.; de Vlieg, J. *Fusarium solani pisi* cutinase. *Biochimie* **2000**, *82* (11), 1015−1021.
(70) Prompers, J. J.; Groenewegen, A.; Van Schaik, R. C.; Pepermans, H. A.; Hilbers, C. W. ^{1}H, ^{13}C, and ^{15}N resonance assignments of *Fusarium solani pisi* cutinase and preliminary features of the structure in solution. *Protein Sci.* **1997**, *6* (11), 2375−2384.
(71) Martinez, C.; Nicolas, A.; van Tilbeurgh, H.; Egloff, M. P.; Cudrey, C.; Verger, R.; Cambillau, C. Cutinase, a lipolytic enzyme with a preformed oxyanion hole. *Biochemistry* **1994**, *33* (1), 83−89.
(72) Burgi, H. B.; Dunitz, J. D.; Shefter, E. Geometrical reaction coordinates. II. Nucleophilic addition to a carbonyl group. *J. Am. Chem. Soc.* **1973**, *95* (15), 5065−5067.
(73) Longhi, S.; Nicolas, A.; Creveld, L.; Egmond, M.; Verrips, C. T.; de Vlieg, J.; Martinez, C.; Cambillau, C. Dynamics of *Fusarium solani* cutinase investigated through structural comparison among different crystal forms of its variants. *Proteins: Struct., Funct., Genet.* **1996**, *26* (4), 442−458.
(74) Arun, A.; Raja, P. P.; Arthi, R.; Ananthi, M.; Kumar, K. S.; Eyini, M. Polycyclic aromatic hydrocarbons (PAHs) biodegradation by basidiomycetes fungi, *Pseudomonas* isolate, and their cocultures: comparative *in vivo* and *in silico* approach. *Appl. Biochem. Biotechnol.* **2008**, *151* (2−3), 132−142.
(75) Austin, H. P.; Allen, M. D.; Donohoe, B. S.; Rorrer, N. A.; Kearns, F. L.; Silveira, R. L.; Pollard, B. C.; Dominick, G.; Duman, R.; El Omari, K.; Mykhaylyk, V.; Wagner, A.; Michener, W. E.; Amore, A.; Skaf, M. S.; Crowley, M. F.; Thorne, A. W.; Johnson, C. W.; Woodcock, H. L.; McGeehan, J. E.; Beckham, G. T. Characterization and engineering of a plastic-degrading aromatic polyesterase. *Proc. Natl. Acad. Sci. U. S. A.* **2018**, *115* (19), E4350−E4357.
(76) Terasaki, M.; Kamata, R.; Shiraishi, F.; Makino, M. Evaluation of estrogenic activity of parabens and their chlorinated derivatives by using the yeast two-hybrid assay and the enzyme-linked immunosorbent assay. *Environ. Toxicol. Chem.* **2009**, *28* (1), 204−208.
(77) Nishihara, T.; Nishikawa, J.; Kanayama, T.; Dakeyama, F.; Saito, K.; Imagawa, M.; Takatori, S.; Kitagawa, Y.; Hori, S.; Utsumi, H. Estrogenic activities of 517 chemicals by yeast two-hybrid assay. *J. Health Sci.* **2000**, *46* (4), 282−298.
(78) Soni, M. G.; Carabin, I. G.; Burdock, G. A. Safety assessment of esters of p-hydroxybenzoic acid (parabens). *Food Chem. Toxicol.* **2005**, *43* (7), 985−1015.
(79) Kamaya, Y.; Tsuboi, S.; Takada, T.; Suzuki, K. J. A. o. E. C. Toxicology, growth stimulation and inhibition effects of 4-hydroxybenzoic acid and some related compounds on the freshwater green alga *Pseudokirchneriella subcapitata*. *Arch. Environ. Contam. Toxicol.* **2006**, *51* (4), 537−541.
(80) Nakagawa, Y.; Moldéus, P. Mechanism of p-hydroxybenzoate ester-induced mitochondrial dysfunction and cytotoxicity in isolated rat hepatocytes. *Biochem. Pharmacol.* **1998**, *55* (11), 1907−1914.
(81) Matthews, C.; Davidson, J.; Bauer, E.; Morrison, J. L.; Richardson, A. P. p-Hydroxybenzoic acid esters as preservatives II. Acute and chronic toxicity in dogs, rats, and mice. *J. Am. Pharm. Assoc., Sci. Ed.* **1956**, *45* (4), 260−267.
(82) Chen, S.; Su, L. Q.; Billig, S.; Zimmermann, W.; Chen, J.; Wu, J. Biochemical characterization of the cutinases from Thermobifida fusca. *J. Mol. Catal. B: Enzym.* **2010**, *63* (3−4), 121−127.
(83) Gmurek, M.; Rossi, A. F.; Martins, R. C.; Quinta-Ferreira, R. M.; Ledakowicz, S. Photodegradation of single and mixture of parabens − Kinetic, by-products identification and cost-efficiency analysis. *Chem. Eng. J.* **2015**, *276*, 303−314.
(84) Golden, R.; Gandy, J.; Vollmer, G. A review of the endocrine activity of parabens and implications for potential risks to human health. *Crit. Rev. Toxicol.* **2005**, *35* (5), 435−458.
(85) Baker, P. J.; Montclare, J. K., Biotransformations using cutinase. In *Green Polymer Chemistry: Biocatalysis and Biomaterials*; American Chemical Society: 2010; Vol. *1043*, pp 141−158.
(86) He, X.; Iasmin, M.; Dean, L. O.; Lappi, S. E.; Ducoste, J. J.; de los Reyes, F. L., 3rd Evidence for fat, oil, and grease (FOG) deposit formation mechanisms in sewer lines. *Environ. Sci. Technol.* **2011**, *45* (10), 4385−4391.
(87) Vieira, M. G. A.; da Silva, M. A.; dos Santos, L. O.; Beppu, M. M. Natural-based plasticizers and biopolymer films: A review. *Eur. Polym. J.* **2011**, *47* (3), 254−263.

DOI: 10.1021/acs.est.8b05275
Environ. Sci. Technol. 2019, 53, 354−364